Adv Polym Sci (2018) 282: 1–34
DOI: 10.1007/12_2017_30

Published online: 28 October 2017

Processing of Poly(lactic Acid)

Ines Kühnert, Yvonne Spörer, Harald Brünig, Nguyen Hoai An Tran, and Natalie Rudolph

Abstract Polymer applications range from biomedical devices and structures, packaging, or toys to automotive and industrial items. So far, biopolymers could replace commodity polymers in a variety of products, especially for biomedical applications or food packaging. One of the most used and widely studied biopolymers is poly(lactic acid) (PLA). To generate new application fields and provide a broader application of PLA, research on processing behavior is still required. This chapter covers the processing relevant behavior of PLA and processing conditions for extrusion melt spinning, injection molding, and additive manufacturing. The processing-related behavior is compared to that of commodity polymers. The aim is to provide an overview of the state of the art and some recent new developments in this research field.

Keywords 3D printing • Additive manufacturing • Crystallization • Injection molding • Interface • Interphase • Mechanical properties • Melt spinning • Morphology • Poly(lactic acid) • Processing • Rheological behavior • Skin-core morphology • Thermal properties • Weld line

I. Kühnert (✉), Y. Spörer, and H. Brünig
Leibniz-Institut für Polymerforschung Dresden e. V., Hohe Straße 6, 01069 Dresden, Germany
e-mail: kuehnert@ipfdd.de

N.H.A. Tran
Institute of Textile Machinery and High Performance Material Technology, Technische Universität Dresden, 01062 Dresden, Germany

N. Rudolph
Polymer Engineering Center, Department of Mechanical Engineering, University of Wisconsin-Madison, 1513 University Avenue, Madison, WI 53706, USA

Contents

1 Poly(lactic Acid) and Its Processing-Related Behavior

1.1 Introduction

Biopolymers (bio-based and/or biodegradable) such as poly(lactic acid) (PLA) are processed and used in the same way as petrochemical-derived polymer materials [1–3]. Morphology development during processing and its correlation with final product properties, together with sketchy long-term behavior, keeps these materials from accelerated market growth [3]. PLA is one of the best known and best understood bio-based materials. Its biocompatibility, biodegradation, and non-toxic behavior makes this material attractive for use as structural parts and also as a functional polymer, for example as an additive in paper materials, adhesives, coatings, thickening agent, flocculants, and concrete agent [1, 2]. In this chapter the processes for manufacturing structural parts and several specific strategies to improve the "structure-process-property" relationship are described.

1.2 Poly(lactic Acid)

The lactic acid monomer for PLA exists in two optically active configurations, namely L-lactic acid and D-lactic acid. Depending on the monomers used and the synthesis reaction conditions, it is possible to control the L-to-D ratio of the final polymer. Therefore, different grades of PLA are available on the market, such as pure poly-L-lactic acid (PLLA), poly-D-lactic acid (PDLA), or PLA with variation of the D content. There are three possible paths for polymerization of lactic acid: direct condensation polymerization, direct poly-condensation in an azeotropic solution, and polymerization through lactic acid formation [4]. As with conventional polymers, a high degree of polymerization and increasing crystallinity lead to an increase in strength, elastic modulus, glass transition temperature (T_g), and melt temperature [5]. According to process parameters, a recrystallization step for the

PLA is set to improve stability against water absorption. In crystalline form, PLA has better chemical stability, and the water resistance and speed of biodegradability are less than for amorphous PLA [5].

Neat PLA shows the following technical properties:

- High Young's modulus
- High scratch resistance
- High transparency
- Certified compostability
- Good printability
- Heat sealability
- High hydrophilicity
- Brittle, low impact strength
- Low heat resistance

To improve the properties and processing behavior of PLA, it is usually compounded and/or blended by the use of different additive packages and fillers. Polymer blends are in general classified into thermodynamically miscible or immiscible blends. Immiscible blends show phase separation and form multiphase structures. Depending on the degree of phase separation of two immiscible polymers, the morphology shows (1) discrete phase-like droplets in the matrix or (2) a bi-continuous phase (co-continuous, matrix-fibrillar structures). From the viewpoint of polymer composites, these structures are in situ reinforced polymer-polymer composites or micro-/nanofibrillar composites [6]. Under certain conditions, the micro- and nanofibrillar structures can be formed during melt processing. Because of the highly hydrophilic behavior of PLA it is recommended that the material be dried before processing. The value of moisture should be less than 0.01 wt% of the total weight to minimize the risk of molecular degradation during processing. For this, PLA resins are packed using moisture-resistant foil liners. The drying condition depends on temperature, time, air flow rate, and dew point. A range of 80–100°C for 4–2 h is recommended for crystalline types. Drying conditions are given in the data sheets of the materials from the manufacturer [4, 7–9].

Some studies of the processing of biomaterials have already been summarized [1–3]. Many academic results exist, and some knowledge has been transferred into industrial applications. Nevertheless, the market growth rate will dynamically increase further in the light of new technology developments (such as in additive manufacturing [AM], melt spinning, and injection molding). A strong driving force is the possibility of controlling structure, especially morphology design, within the product [2, 5, 10–15].

1.3 Processing-Related Behavior of PLA

To understand processing behavior, knowledge of the rheological, thermal, and thermodynamic (pressure-volume-temperature [pvT]) properties of PLA is important [1]. The crystallization behavior of PLA was studied in several investigations

[16–22]. Consequently, the thermal behavior, melting, and crystallization under processing conditions are discussed in detail in the following section. Only a few studies are available regarding rheology and pvT behavior [12, 23, 24], and these are discussed later in Sects. 1.3.2 and 1.3.3.

1.3.1 Thermal Behavior

A typical method to determine thermal properties of polymer materials is differential scanning calorimetry (DSC) [25, 26]. During measurement the sample and a reference are heated and cooled with defined heating and cooling rates, respectively. The differential heat flow is measured, which is proportional to the thermodynamic transformation during melting or crystallization. In contrast to semi-crystalline polymers, for amorphous polymers only T_g can be established. Semi-crystalline polymers show characteristic melting and crystallization behaviors, which, depending on their molecular structure, result in the formation of a detectable heat flow peak. From these peaks the melt and crystallization temperature can be determined. The results can be used to calculate the degree of crystallinity depending on the cooling rate, the crystallization growth rate, and the crystallization temperature. Altogether, these data are important for choosing the right process parameters.

Investigations by Iannace et al. [17] on the isothermal crystallization behavior of PLA have shown that the crystallization growth rate has a maximum which depends on the isothermal crystallization temperature. During these studies, PLA was melted at 200°C for 2 min, cooled down to defined temperatures (90, 110, and 130°C), and then crystallized for 30 min at these temperatures. Following the crystallization, the samples were heated again to 200°C at 10°C/min and the heat flow was measured simultaneously. The influence of cooling condition (cooling rate) was not given. They [17] concluded that the crystallization rate shows a maximum around 105°C and that high undercooling leads to incomplete crystallization. Upon reheating, exothermic crystallization behavior occurs close to the melting point. The presence of amorphous fractions, which do not relax at T_g, was observed. Below 110°C the number of amorphous regions was higher than above 110°C, which means that a regime transition occurs. Similar conclusions were also made in [19, 20]. The crystallization behavior of PLLA using DSC measurements to determine isothermal and non-isothermal thermodynamic behavior was investigated. They reported a discontinuity in crystallization growth at around 116–118°C, resulting in a bell-shaped curve for crystallization growth rate as a function of crystallization temperature. This is shown in Fig. 1, where T_b is the boundary temperature between the low- and high-temperature ranges [20]. The results indicate a difference in the crystallization mechanism between the high and the low temperature values caused by different crystal modifications, which have been reported in various studies [18, 27–29]. Investigations by Miyata [18] have also shown that the crystallization growth rate increases with decreasing average molar mass, M_W [30].

Figure 2 shows the heating curves of PLLA with varying processing history. PLLA was injection molded into a cold mold, which promotes fast cooling

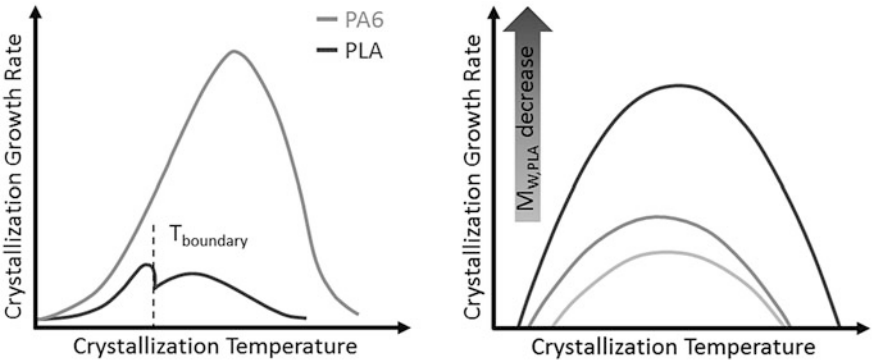

Fig. 1 Bell-shaped crystallization growth curves as a function of isothermal crystallization temperature: (*left*) PLA [according to 20] compared to PA6 [according to 31]; (*right*) PLA varying in the molecular mass [according to 18] (modified with permission of Elsevier and AIP)

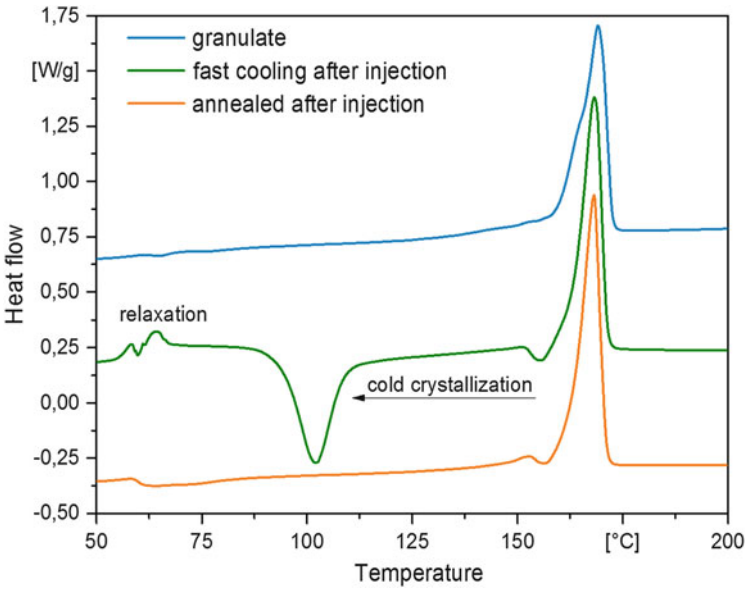

Fig. 2 Heating curves from PLLA after processing. Heating rate 10°C/min and using normal DSC. (Data source: Leibniz-Institut für Polymerforschung Dresden e. V.)

especially on the surface of the molded part. After ejection, the molded parts were optically amorphous and some parts were annealed at 100°C for 24 h. From all injection molded samples, DSC measurements were carried out using a heating and cooling rate of 10°C/min. A cold crystallization peak around 100°C was observed during heating, indicating that macromolecular chains are frozen in their orientation because of the rapid cooling during injection molding. These frozen molecular chains are able to relax and crystallize at temperatures higher than T_g ($T_g = 60$°C).

Annealing after injection molding occurs with the disappearance of the cold crystallization peak, indicating that the formation of crystallites takes place during this annealing time.

During injection molding, cooling rates of more than 1,000°C/s at the polymer/mold interface can occur. To simulate these high cooling rates, fast scanning calorimetry could be used, as is shown in literature for PLLA [32, 33], as well as for other polymers [34, 35].

1.3.2 Flow Behavior

To determine the flow behavior of polymers, the relationship between shear stress and shear rate can be established using rheometers, such as rotational and capillary rheometers [36]. During these measurements, shear strain is induced to determine the viscosity at different temperatures.

Figure 3 shows the influence of shear rate on the viscosity of different PLA types at their average processing temperature (left image) and of PLA 3251D as a function

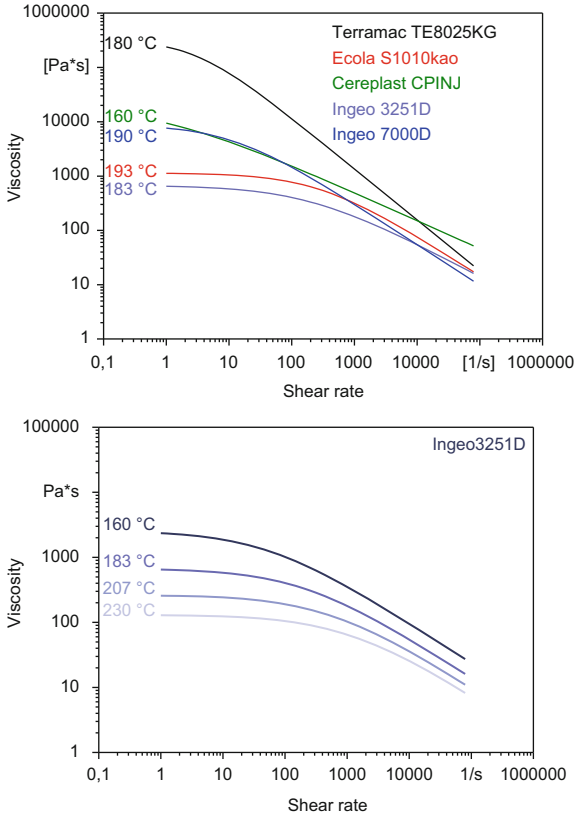

Fig. 3 Comparison of Moldflow data of viscosity vs shear rate: (*left*) different types of PLA at processing temperature; (*right*) PLA3251D at different temperatures. (Database: Moldflow™, Cadmould, Leibniz-Institut für Polymerforschung Dresden e. V.)

of the temperature (right image). As can be seen, the different types of PLA show different rheological behavior because of their molecular structure. With an increase in temperature (right), the free volume between the molecular chains increases and the intra-molecular friction decreases. This behavior results in the lowering of the viscosity. It is also known that an increase in molecular weight occurs in a shift of the shear rate independent plateau to higher viscosity values [37].

1.3.3 pvT Behavior

pvT measurements are used to describe the thermodynamic behavior of the specific volume, v, as a function of pressure, p, and temperature, T. The data are used to evaluate the processing parameters, especially for injection molding. However, the measurements are carried out using slow heating, and cooling rates are therefore far from real processing conditions.

Amorphous and semi-crystalline polymers show different thermodynamic behavior as shown in Fig. 4. The pvT diagrams show the thermal expansion and specific thermal transitions of polymers [23, 24]. Amorphous polymers such as polycarbonate or polymethylmethacrylate show primary glass transition, T_g, behavior, where T_g is clearly the temperature where the polymer changes from solid to molten state. For semi-crystalline polymers the behavior is different and the pvT diagrams show a transition area in which the polymers maintain structural continuity up to the temperature where the crystals melt. As can be seen in Fig. 4, for PLLA this transition area only occurs at low pressure. However, it is important to note that the cooling rates during these measurements are very slow (1°C/min). During cooling at high pressure the curve shape assumes a more and more amorphous character, which means that the material becomes solid before crystallization takes place.

To visualize the process-material relation, the pvT diagram can be used. In this diagram the thermodynamic changes of the thermoplastic material and the process data of average part temperature together with the pressure development taken from in-mold pressure measurements during the injection process can be correlated. Finally, all previously discussed material data are basically necessary to reach the optimal process window for the required product properties.

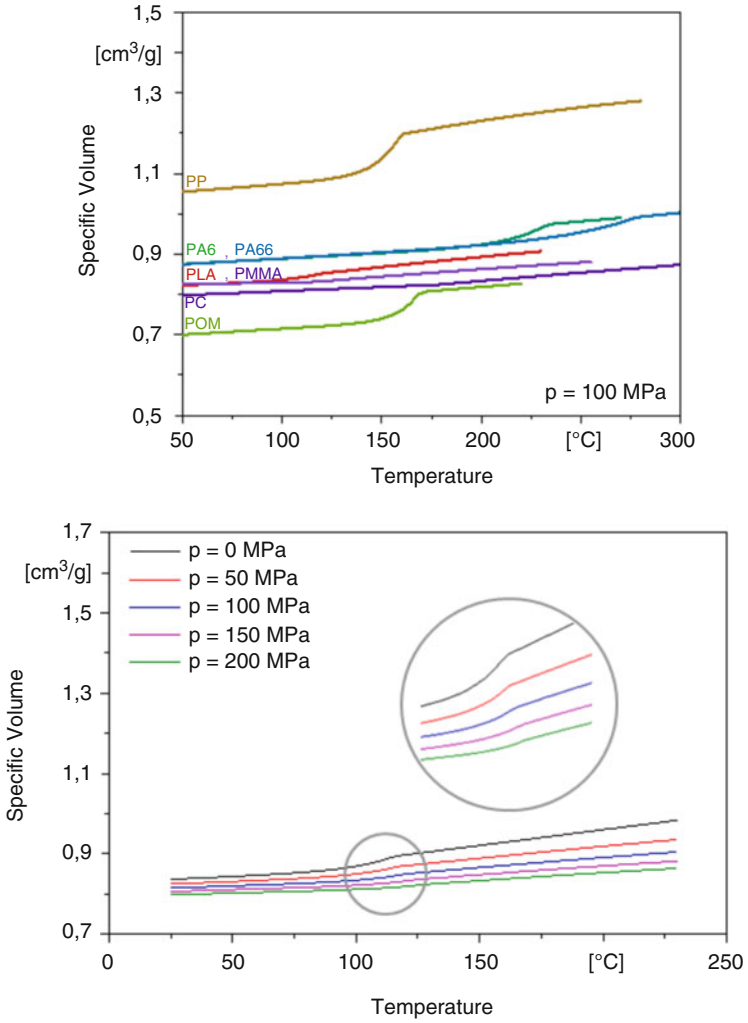

Fig. 4 Comparison of Moldflow data of pvT behavior with specific volume vs temperature and pressure: (*left*) PLA in comparison to other semi-crystalline and amorphous polymers; *right*) PLA under variation of pressure conditions. (Database: Moldflow™, Cadmould)

2 Insights into the Processing of PLA

2.1 Extrusion

The extrusion process is characterized by the continuous melting, conveying, and discharge of plastic materials through a die. Therefore the typical single screw is divided into feed, transition, and metering sections as shown in Fig. 5. Process

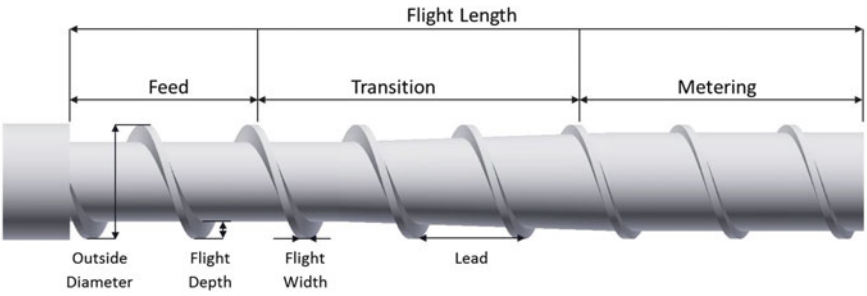

Fig. 5 Extrusion single screw plasticizing unit scheme. (Data source: Leibniz-Institut für Polymerforschung Dresden e. V.)

relevant screw parameters are the L/D ratio and the compression ratio. The L/D ratio is the ratio of flight length to the outer diameter of the screw. The compression ratio is defined as the ratio between the flight depth in the feed section and in the metering section. For PLA, L/D ratios of 24–30 and compression ratios of 2–3 are recommended [38–40].

The plasticizing of PLA starts at the conveying zone with movement of the polymer pellets or powders from the hopper to the screw channel. Inside the channel the rotating screw transports the compacted material down the channel, and the material is sheared and pushed against the barrel wall. Because of the friction during transport through the transition zone, the material melts. Heat bands are wrapped around the outside of the barrel. The thermal energy from the heater combined with frictional heat from the material transport leads to temperatures above the melting point of the PLA ($T_M = 170–180°C$) [1]. The temperature of the heater is usually set to 200–210°C [1] to ensure the deletion of thermal history of the material and that no crystalline structures remain. The size of the solid bed shrinks during the melting of material and a melt pool is formed. After the transition zone, the melt passes into the metering zone, where sufficient pressure is generated to pump the material through the die [1, 41].

Extrusion is used as a shaping process in blow molding and film blowing processes, in which the melt is discharged through a special shaped die. For these processes, a high melt stiffness is required to ensure film stability and a continuous process cycle. In the case of PLA, the melt strength is low and needs to be improved to enlarge the processing window and application field. Therefore, during the last few years, several possibilities have been reported to enhance the melt properties of PLA, dealing primarily with chain modification of PLA [42–48]. Furthermore, the extrusion process plays an important role as plasticizing unit for melt spinning [49–54] and injection molding [5, 55–61].

2.2 Melt Spinning

2.2.1 Introduction

Melt spun PLA fibers from renewable sources are in many cases an alternative for replacement of petroleum-based synthetic fibers, although the requirements regarding thermal stability and rheological flow behavior for the polymeric materials used for melt spinning are high. Two important advantages of the melt spinning process are: (1) the process is environmentally friendly because there are no solvents needed and (2) melt spinning can be done with high productivity, especially by using the high speed spinning process.

The majority of publications focus on melt spinning of PLA and the best results were found using PLA with low D content (lower than 2%) [45].

It is known from injection molding dogbone specimens that PLA parts typically show high brittleness and low elongation at break. However, material processed by a melt spinning process is quite different. Because of the high deformation rate and tensile stress within the spinning line, orientation of the polymeric chains occurs and their crystallization into fibrillary structures is possible. Orientation and crystallization mechanisms allow the producer to adjust significantly the mechanical properties of melt spun PLA fibers. Depending on the spinning conditions, the fibers show elongation at break between 20% (high oriented at maximum possible draw ratio) to 300% (for low speed spinning without drawing), maximum tenacity (tensile strength) up to 35–40 cN/tex[1] (~450–500 MPa), and elastic tensile modulus 2–6 GPa. On account of similarities between PLA fiber properties and their processing behavior with polyethylene terephthalate (PET), the PLA can be processed on existing spinning equipment (filament yarns, staple fibers, spun-bonded nonwovens) [49].

The first laboratory investigations into PLA fiber spinning were carried out with low take-up velocities (lower than 10 m/min). Later, high speed spinning and drawing process conditions were investigated using close to industrial scale extruder spinning equipment [50]. Today, the global production capacity of PLA is ~700,000 tons/year [62] and PLA fiber spinning is now a well-established industrial process.

2.2.2 Properties of PLA Fiber-Grade Pellets

Melt spinning (especially high speed spinning) requires high purity and homogeneity in the primary material. PLA materials differ with respect to their D/L-lactic content, their molecular weight M_w, and their molecular weight/number ratio (M_w/M_n). Typical values for easily spinnable PLA grades are small content of D-lactic (<5%), a molecular weight in the range of M_w = 250,000–450,000 g/mol

[1] tex is the measure of fineness in textiles (linear density), a fiber has the fineness 1 tex when 1,000 m of fiber length weight 1 g: 1 tex = 1 g/1,000 m.

and a narrow molecular weight distribution ($M_w/M_n = 2–2.5$). Table 1 shows some further properties in comparison with other fiber-forming polymers.

To prevent viscosity/molecular weight degradation during melt spinning, a moisture content of less than 0.005% is recommended. Most drying systems operate using nitrogen or under vacuum.

2.2.3 Melt Spinning of PLA: Process Parameters

Multifilament yarns can be manufactured using melt spinning equipment as shown schematically in Fig. 6. The dried PLA pellets (dried, for example, at 120°C under

Table 1 Comparison of properties of PLA resins with other fiber-forming melt-processable polymers [51]

Property	PLA	Polypropylene	PET	Polyamide
Density (g/cm^3)	1.26	0.92	1.38	1.14
T_g (°C)	55–60	(12–20)	90–100	40–45
Melting temperature (°C)	165–180	175	265	214
Moisture content (%)	0.5	–	0.4	4.5
Heat value (kJ/kg)	19,000	40,000	23,000	31,000

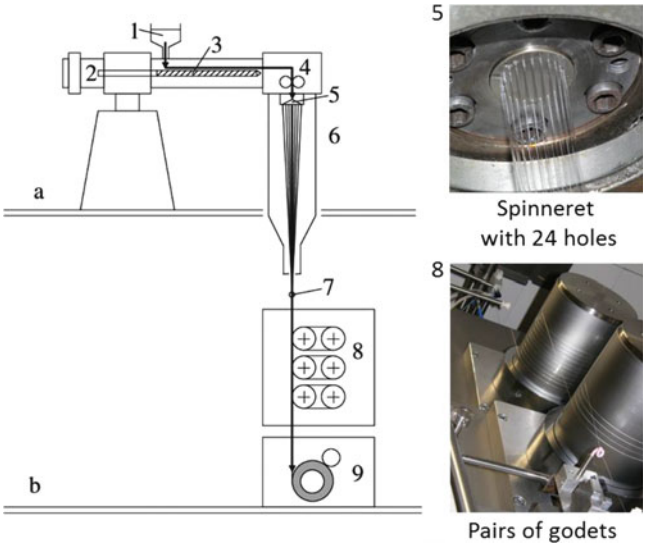

Fig. 6 Melt spinning equipment (schematic): (**a**) spinning floor; (**b**) winding floor. (1) Container with polymer pellets, (2) electric motor and drive train, (3) extruder assembly with screw, (4) spinning head with metering pump (gear pump), (5) spinneret with capillary holes, (6) spinning chamber with quenching air, (7) spin finish applicator, (8) pairs of (heatable) godets for online drawing, (9) (high speed) winder. From [52]; corresponds to the melt spinning equipment at Leibniz-Institut für Polymerforschung Dresden e. V.

vacuum for 16 h using a drum dryer) are fed under nitrogen atmosphere into the container (1). Typical dimensions of the extruder screw (3) are 20–40 L/D ratio. The use of a mixing tip and/or a static mixer can be advantageous for creating a uniform melt temperature.

Typical conditions and parameters for the melt spinning of multifilament PLA yarn at Leibniz-Institut für Polymerforschung Dresden e. V. are described below (see Table 2). The extruder zone temperatures and the temperature of the spinning head have to be adapted to the melting temperature of PLA and to its rheological flow behavior. To support a stable spinning process, the viscosity of the melt in the spinneret should be in the range of 100–500 Pas, and the melt pressure should not exceed 50–80 bar.

It is possible to realize the melt spinning procedure with or without an *online* drawing step by godets (as seen in Fig. 6) or with an additional *offline* drawing step after winding the yarn on bobbins at a separate drawing machine.

2.2.4 Mechanical Properties of Fiber Yarns

Figure 7 shows typical results of the mechanical property, tensile strength, as a function of elongation, for three different variants of PLA melt spinning with moderate online drawing. All samples are wound at 3,000 m/min. The values for elongation at break, maximum tensile strength, and Young's modulus are in the ranges of 45–65%, 23–25 cN/tex, and 300–400 MPa, respectively.

An additional offline drawing procedure can be used to improve the yarn's mechanical properties. These external drawing steps increase the orientation as well as the crystallinity of the PLA fiber material, resulting in a reduction of fineness and higher maximum tensile strength (tenacity), higher elastic modulus (Young's modulus), and lower elongation at break. Figure 8 shows the force-elongation behavior of a PLA filament yarn (125 dtex f6) after an offline drawing process with different DR. In this case, a maximum tensile strength of ~30 cN/tex

Table 2 Parameters of melt spinning of PLA. (Data source: Leibniz-Institut für Polymerforschung Dresden e. V.)

Polymer	PLA 6002D (NatureWorks® LLC)
Pellets preparation	Drying at 80°C, 16 h, vacuum
Extruder screw diameter, L/D-ratio	18 mm, 25
Extruder zone temperatures	25, 180, 200, 230, 235, 235°C
Melt temperature	235°C
Spinning pump, mass throughput	18 g/min
Spinneret, number of holes Capillary diameter, L/D ratio	12 0.3 mm, 2
Quenching chamber, length Cooling air: temperature, profile	1.5 m 16°C, 0.25 m/s
Take-up velocity, 1st godet	1,500, 2,000, 3,000 m/min
Draw ratio (online)	1.0–3.0
Temperature of drawing godets	80–120°C
Winding speed	3,000–4,500 m/min

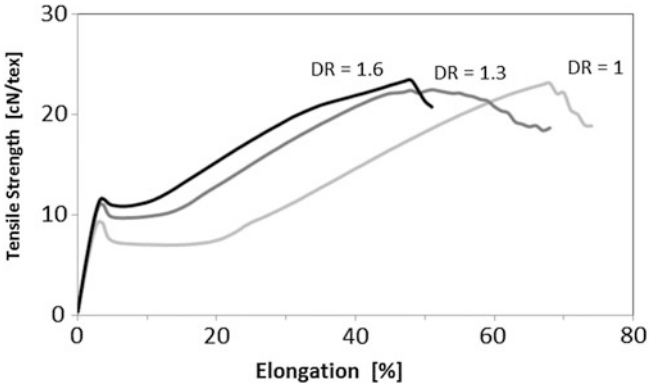

Fig. 7 Tensile strength vs elongation for three different variants of PLA melt spun and online drawn fiber yarns. Online draw ratios (DR) = 1.6, 1.3 and 1.0 (no drawing, for comparison), winding speed: 3,000 m/min, yarn fineness 60 dtex f12. (Data source: Leibniz-Institut für Polymerforschung Dresden e. V. [63])

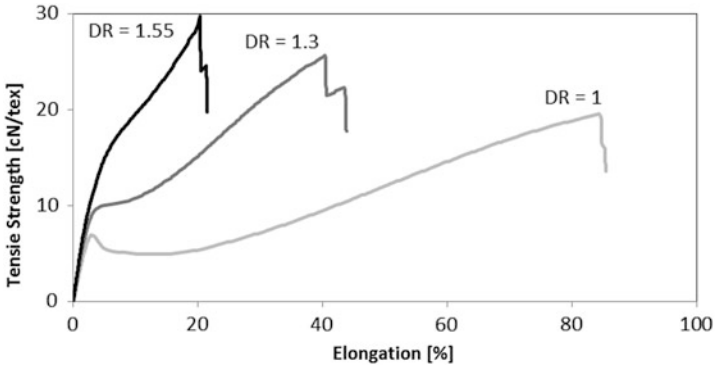

Fig. 8 Tensile strength vs elongation for three different variants of PLA melt spun and offline drawn fiber yarns. Basic yarn fineness: 125 dtex f6, offline DR = 1.55, 1.3, and 1.0 (no drawing, for comparison), fineness after drawing: 97 and 80 dtex f6. (Data source: Leibniz-Institut für Polymerforschung Dresden e. V. [63])

(ca. 375 MPa), an elongation to break of 20%, and an elastic modulus of ~600 MPa was reached for the highest DR = 1.55.

The applied tensile stress is one of the most essential variables for the fiber formation process during the spinning and drawing procedure. The higher the stress the higher the orientation of the polymer chains, which leads to a higher degree of crystallization. This in turn normally leads to improved mechanical properties. However, frozen-in tensions typically cause the thermal shrinkage of the fiber yarns, which is in most cases unwanted. To optimize yarn properties and to reduce internal tensile stress, the producers balance the relaxation by thermal treatment. Figure 9 shows, for example, the shrinkage behavior of a highly

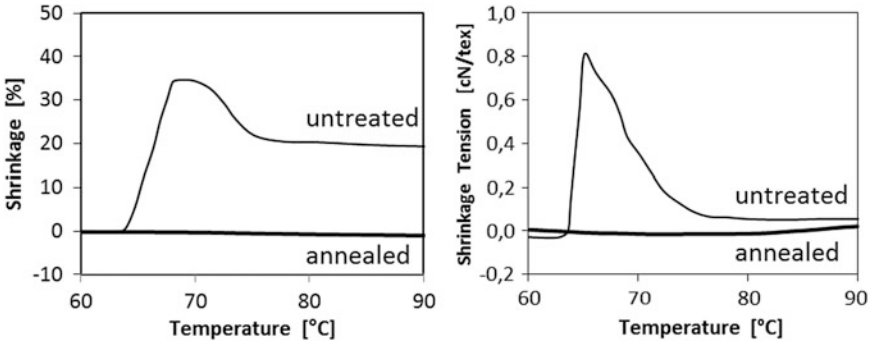

Fig. 9 Shrinkage tension (*left*) and shrinkage (*right*) vs temperature of different thermal treated PLA fiber yarns. The shrinkage of the untreated yarn (*upper curves*) starts at 65°C; the tempered yarn (*lower curves*) shows practically no shrinkage. (Fineness: 480 dtex f48, pre-tension: 0.2 cN/tex, heating rate: 20 K/min). (Data source: Leibniz-Institut für Polymerforschung Dresden e. V. [64])

oriented PLA fiber yarn before and after an additional thermal treatment (annealing at 80°C for 1 h).

2.2.5 Filament and Fiber Yarns

Besides mechanical and thermal properties, the number of single filaments and their fineness are also important for the textile performance of the fibers. Another essential aspect for properties such as tactility, grip, comfort, pilling propensity, etc., is the cross-sectional shape of the single filaments. The most common are fibers of circular cross sections because spinnerets with circular capillary holes are easier to manufacture. Figure 10 schematically shows the cross section areas of melt spun PLA fiber yarns with similar total fineness. Although these yarns are similar in their total fineness and force-elongation characteristics, their tactility and bending is quite different.

For melt spinning of non-circular, profiled, or hollow fibers, custom-built spinnerets with capillary holes corresponding to the desired geometry have to be used. Figure 11 shows examples of profiled capillary holes and Fig. 12 shows the melt spun PLA fiber yarns from these spinnerets with different cross-sectional shapes. All single filaments in Fig. 11 have the same fineness of 5 dtex.

The cross-sectional area of the single filaments in Fig. 12 is equal for each sample; the perimeter and therefore also the fiber surface area increases from left to right. Another criterion for the deviation of the cross section of profiled fibers from circular fibers is the so-called "circularity", $C = 4\,\pi\,A/P^2$, with A = cross-sectional area and P = perimeter. Table 3 shows the values for perimeter and circularity for the different fiber shapes.

It can be seen that the perimeter and therefore the surface area of the cruciform fibers is about twice as large as those of the circular fibers. Designing the surface area is an interesting aspect for biomedical applications, for example, for wound covering or absorbing applications. Besides the mechanical properties, the

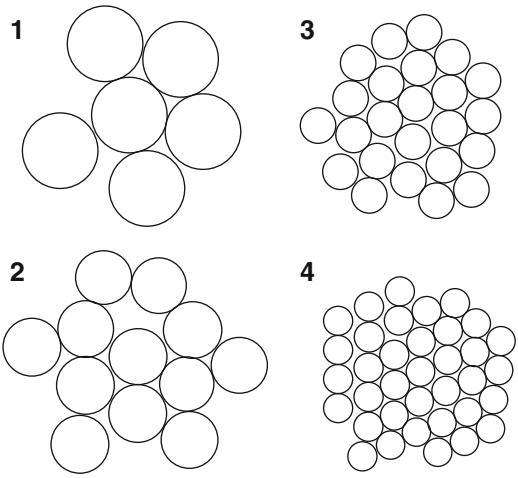

Fig. 10 Comparison of the cross section area of melt spun PLA filament yarns with different numbers of single filaments and different filament diameters (schematic). (1) 150 dtex f6 (single filament diameter 48 μm), (2) 160 dtex f12 (diameter 36 μm), (3) 120 dtex f24 (diameter 22 μm), (4) 120 dtex f36 (diameter 18 μm). (Data source: Leibniz-Institut für Polymerforschung Dresden e. V.)

Fig. 11 Three different cross-sectional shapes of the capillary holes of the spinneret (trilobal short, trilobal long, cruciform); bar 200 μm. (Data source: Leibniz-Institut für Polymerforschung Dresden e. V.)

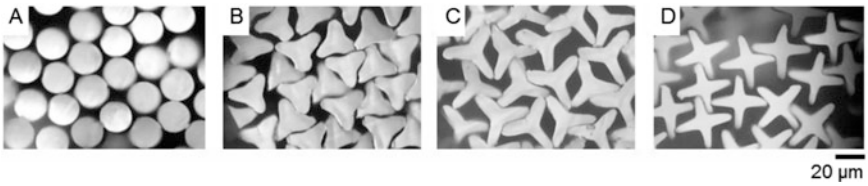

Fig. 12 Cross-sectional shapes of PLA fiber yarns spun with spinneret holes from Fig. 10. Total yarn fineness: 60 dtex f12, single filament fineness: 5 dtex. (**a**) Circular (for comparison); (**b**) trilobal short; (**c**) trilobal long; (**d**) cruciform; bar 20 μm. (Data source: Leibniz-Institut für Polymerforschung Dresden e. V.)

Table 3 Perimeter *P* and circularity *C* of profiled fibers (see Fig. 11)

Shape of fiber	Perimeter (μm)	Circularity C (−)
A – circular	71	1.0
B – trilobal small	92	0.61
C – trilobal long	126	0.33
D – cruciform	139	0.26

biocompatible and biodegradable behavior also plays an important role for medical applications. Tissue engineering based on biocompatible materials is considered as one alternative approach for cell-seeded, three-dimensional scaffold structures. Herewith, textile manufacturing allows the fabrication of structures with adapted mechanical properties based on resorbable and biocompatible PLA fiber materials with a defined degradation behavior. PLA fibers have therefore been investigated for several tissue engineering applications, for example, the anterior cruciate ligament [53, 65, 66]. The challenge is to realize the specific mechanical requirements for the ligament structure together with biocompatibility and a guarantee of high medical standards (e.g., sterilization).

2.2.6 Melt Spinning of PLA Blends, Microfibrillar and Nanofibrillar Structures

A novel and simple fabrication process for producing biodegradable and biocompatible nanofibrillar PLA structures from blends of PLA and poly(vinyl alcohol) (PVLA) has been developed using the conventional melt spinning method [54, 67, 68]. It was found that the as-spun and drawn PLA/PVLA filaments have sufficient strength for further processing in various textile processes such as weaving or knitting. After textile processing, the water soluble PVLA matrix component can be dissolved and the nanofibrillar PLA structures remain (see Figs. 13 and 14).

To sum up, melt spinning of PLA results in fiber yarns with excellent textile and environmental properties. There is a wide spectrum for medical applications, packaging, hygiene products, textile clothing, and houseware. The production processes of high speed spinning and drawing, staple fiber spinning, and spunbonded nonwovens are well established. Composite materials and/or micro- and nanofibrillar structures can also be produced. However, PLA fibers, so far, have played a limited role in the textile market with respect to market volume and in comparison to oil-based materials.

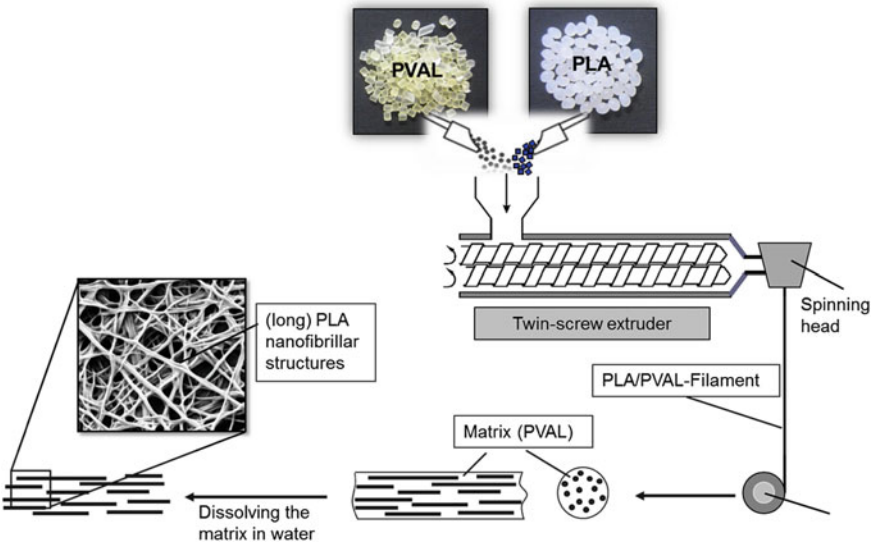

Fig. 13 Melt spinning of nanofibrillar PLA structures from PLA/PVLA blends (schematic)

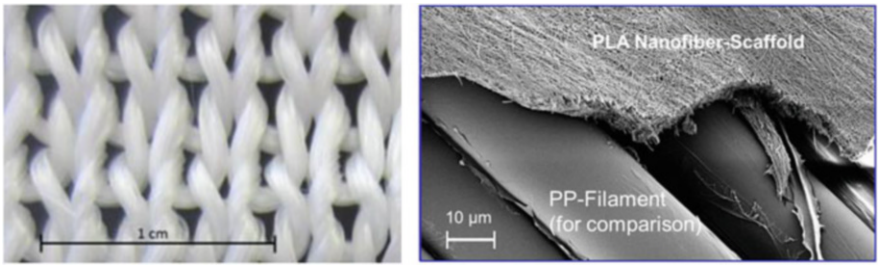

Fig. 14 Knitted fabric from PLA/PVLA 30/70 blend (*left*) and PLA nanofiber scaffold after removing PVLA matrix (*right*). (Data source: Leibniz-Institut für Polymerforschung Dresden e. V. [68])

2.3 Injection Molding

2.3.1 Introduction

Injection molding is one of the most used processing methods for polymers, and also for PLA [1–3, 55]. This economic technology plays an important role in the fabrication of complex parts and mass-produced articles. The main advantages of injection molding are: (1) the direct route from the raw material to the finished part, (2) no or minor post-processing, (3) the possibility of fully automated processing, and (4) high reproducibility and precision. There is no extra injection molding machine configuration for PLA. A common plasticizing unit with a three zone screw to melt the material mainly by friction heating is used. In the same way as for all usual thermoplastics, the thermal management of injection molds works on the assumption that the cycle has to be as short and effective

as possible. Therefore, the mold is tempered at a low temperature to transfer the heat away from the cavity and cool the part down rapidly. Cooling rates are controlled by the ratio between melt and mold temperature, whereby a high cooling rate leads to more characteristic skin-core-like morphology, as is well known from semi-crystalline materials. The skin has a small crystalline morphology that seems amorphous viewed under an optical microscope. In the core the morphology is formed with larger crystalline structures such as spherulites because of the longer remaining time under heat [69].

2.3.2 Influence of Processing Conditions on Structure-Properties Behavior

Injection Molding Process

The injection molding process is divided mainly into eight steps as shown in Fig. 15 [41, 69]. An injection cycle starts with the closing of the mold. In the next step the thermoplastic polymer melt is injected into the mold cavity that is tempered far below the solidification temperature of the polymer. To achieve the filling of the cavity, the screw moves forward until it has moved the required volume of material. During injection the molecular chains are oriented in the flow field by elongational and shear stresses, which lead to specific structure-property effects. After the filling procedure, a holding pressure is maintained to compensate for material shrinkage until the material in the gate solidifies and no additional melt can be pushed into the cavity. The shrinkage is enhanced by the

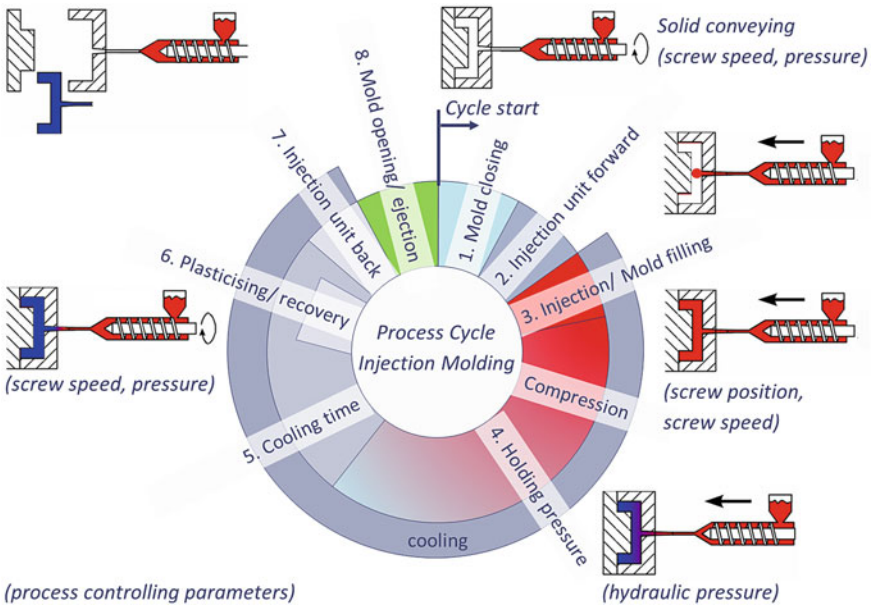

Fig. 15 Scheme of the injection molding process cycle. (Data source: Leibniz-Institut für Polymerforschung Dresden e. V.)

cooling process of polymer materials, in particular when crystallization occurs and the density increases rapidly. After the holding pressure is applied, the part further cools down in the mold and the screw turns back, conveying and melting the material for the following shot. When the injection molded part is sufficiently cooled, the mold opens and the molded part can be ejected. The whole cycle time is calculated from the mold closing until the ejection of the mold part, with the cooling step taking up most of the cycle time.

Crystalline Morphology and Properties

During the injection molding process, the morphology and the thermal and mechanical properties of PLA are influenced by the processing parameters. Important processing parameters are melt temperature (T_m), mold temperature (T_W), injection flow rate (Q_{inj}), holding pressure (P_h), and resulting parameters such as maximum shear rate ($\dot{\gamma}$) and shear stress (τ_W).

The influence of different parameter settings has already been investigated for PLA amongst others [3, 13, 14, 55–57]. In these studies, morphological characterization techniques such as the hot recoverable strain test (HR) to determine the initial level of molecular orientation in molded samples, and differential scanning calorimetry (DSC) to determine the crystallinity degree X_C in injection molded parts were used. The HR describes the difference between the sample dimension before and after thermal treatment. Figure 16 gives an overview of the results and the processing-

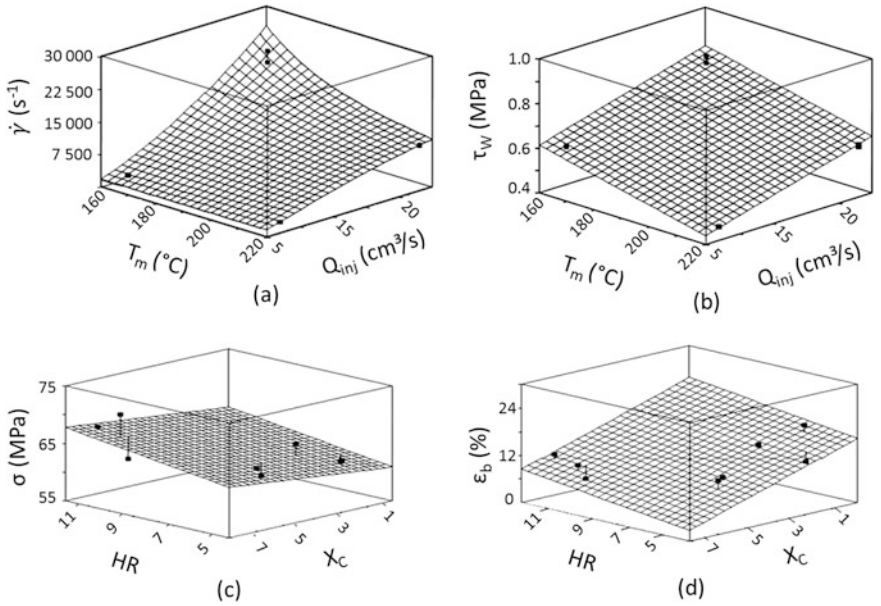

Fig. 16 Overview of processing-property relationships in injection molded PLLA [55]. (**a**) Maximum shear rate $\dot{\gamma}$ as function of the injection flow rate Q_{Inj} and processing melt temperature T_m. (**b**) Maximum shear stress τ_W as function of the injection flow rate Q_{Inj} and processing melt temperature T_m. (**c**) Maximum yield stress σ as function of the hot recoverable strain HR and the crystallinity X_C. (**d**) Elongation at break ε_b as function of the hot recoverable strain HR and the crystallinity X_C. (With permission of Wiley)

property relationship of injection molded PLLA [55]. In [55] the injection parameters (melt-, mold temperature, holding pressure) were systematically changed and the thermomechanical environment for the mold filling phase was simulated. From the received data the shear stress and shear rate were calculated. The melt temperature T_m and the injection speed Q_{Ing} control the shear rate $\dot{\gamma}$ and shear stress τ_W during filling of the cavity, which respectively influence the hot recoverable strain HR and the crystallinity X_C. Low T_m values and high Q_{Ing} facilitate a high level of $\dot{\gamma}$ and τ_W (Fig. 16a, b) occurring in molecular orientation and high crystallinity degree. Both the orientation and crystallinity influence the tensile strength σ and elongation at break ε_b (Fig. 16c, d). An increase in molecular orientation and crystallinity occurs in a maximum σ, whereas an increase in orientation and decrease in crystallinity occur in a high ε_b.

Recent optical investigations on thin sections of injection molded tensile bars using polarized light have also shown large amorphous regions in which crystallites in the form of single spherulites are found, as can be seen in Fig. 17. In this case, semi-crystalline PLA could be produced without further additives. The sample was prepared using a slow cooling condition at a mold temperature of 100°C for 10 min. Samples prepared at normal processing conditions (high cooling rate, fast cycle time) stayed amorphous. From the first heating curve of DSC measurements from the molded parts, a crystallization degree of 26% could be observed; see Fig. 18.

Process Influence on Crystallinity

In [55, 56] it is described how the crystallinity in injection molded parts can be improved by chain orientation achieved because of the shear stress during the injection process or by the addition of nucleating agents. Typical nucleating agents are fillers such as talc and PDLA to form stereo-complex crystals [13, 14, 70, 71]. Another study from [56] also focused on the influence of an alternative injection technique, shear controlled orientation in injection molding (SCORIM) on molecular orientation and mechanical properties of PLLA. SCORIM is used to improve molecular orientation compared to the conventional injection molding process and also to improve weld lines in parts. Using the SCORIM technique, the melt inside the cavity is pushed and pulled until the melt is solidified. During this process the molecules are oriented in the flow direction layer by layer. By using the push and pull effect the melt state, in-mold

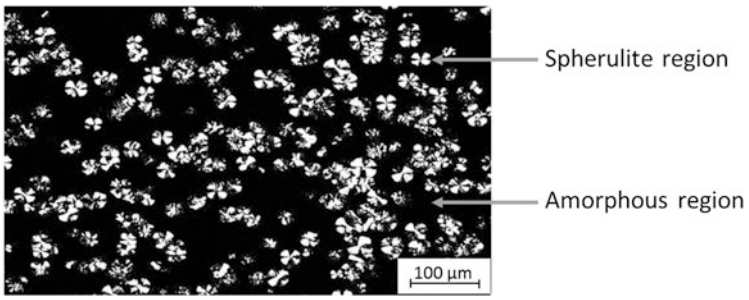

Fig. 17 Observed single spherulites after injection molding process using polarized light microscopy. (Data source: Leibniz-Institut für Polymerforschung Dresden e. V.)

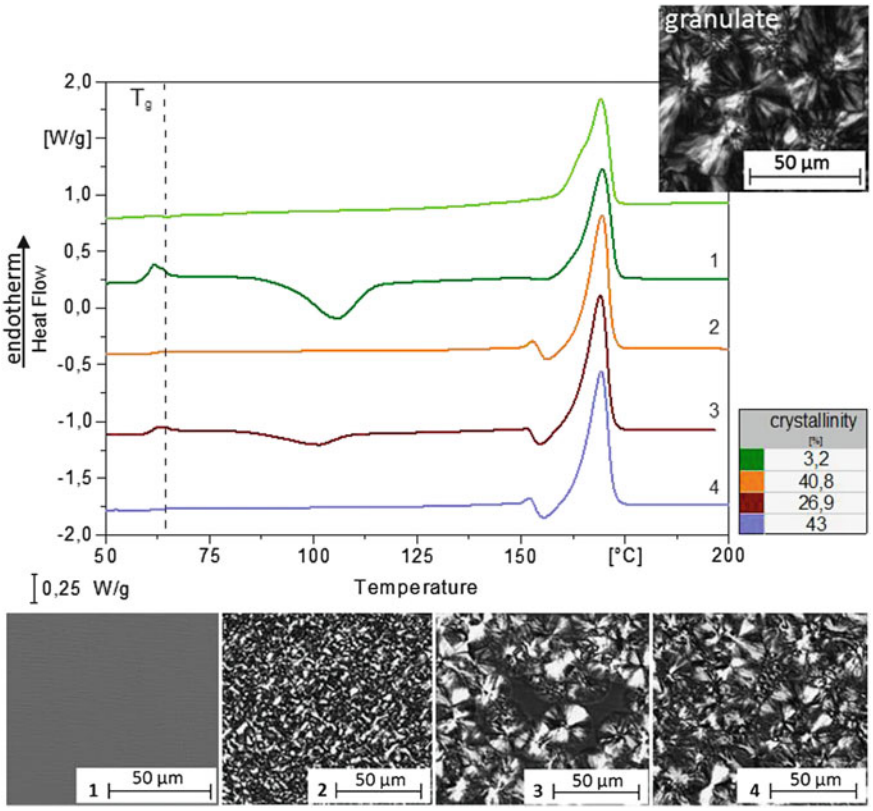

Fig. 18 DSC-first heating curves made from thin cuts of injection molded samples under various process conditions. (1) Amorphous after injection into a cold mold cavity, (2) crystalline after annealing the sample of 1 at a temperature over the T_g for 24 h, (3) crystalline after injection into a hot mold cavity, (4) crystalline after annealing the sample 3 at a temperature over the T_g for 10 min. (Data source: Leibniz-Institut für Polymerforschung Dresden e. V.)

shearing, and cooling can be controlled and thereby the morphology and mechanical behavior, in particular the toughness and maximum stress, can be improved.

Another promising way to improve the crystallinity of PLA is to build PLLA/PDLA stereo-complexes [14]. Common methods are solution casting and melt blending, which are environmentally damaging because of the usage of organic solvents and the degradation of homopolymers at the required blending temperature, respectively. Srithep et al. [14] show the possibility of hand mixing PLLA/PDLA and the effect of molding temperatures on thermal and mechanical properties in injection molded PLLA/PDLA parts compared to pure PLLA. The blend was compounded with 50 wt% PLLA and 50 wt% PDLA. The authors concluded that stereo-complexation improved the elongation at break and storage modulus as well as the crystallization rate, in comparison to pure PLLA. Other investigations have proved the influence of PDLAs varying in their structure [72] and the addition of modifiers by chemical

crosslinking [12] on the rheological and thermal behavior of PLA. The PLLA/PDLA blends showed solid-like viscoelastic behavior at low temperature and the crosslinking density follows a specific order attributed to the stereo-complex crystallites. Investigations on the crystallization behavior [72] have shown that the nucleation mechanism and crystal growth dimension are directly affected by PDLA structure, crystallization temperature, and thermal treatment. Yamoum et al. [12] followed another way and concluded that crosslinking structures can be introduced into PLA by initiation of dicumyl peroxide (DCP) and the presence of crosslinking agents such as bisphenol A ethoxylate dimethacrylate (BIS-EMA). Crosslinked PLAs reveal an improvement in storage modulus and viscosity, and showed a decrease in thermal properties with increasing content of BIS-EMA.

As well as the shear stress during injection molding, crystallinity can also be influenced by tensile strain. The effect of nucleating agents on strain-induced crystallization of PLLA was investigated by Yin et al. [71]. Injection molded specimens were stretched under isothermal conditions (75°C) using a hot stage and the molecular orientation was measured in situ via X-ray scattering. It could be concluded that the crystallinity of nucleated PLLA after uniaxial stretching can be enhanced in the following sequence:

$$\text{talc} < \text{PDLA} < \text{PDLA/talc}$$

The PDLA blends have existing physical crosslinks that are formed by stereo-complex crystals which are a possible reason for faster strain hardening. To eliminate the effect of plastic deformation of formed crystallites, isothermal crystallization after step strain at high stretching speed was performed [71].

2.3.3 Formation of Interfaces

Because of the usual complexity of injection molded parts, multiple gates are often required or the melt flow has to go around mold inserts (flow obstacles). Such design is unavoidable to form those parts. During the injection molding processes, different types of interfaces can occur, such as weld lines [58, 61, 73–75]. Weld lines are well known in any thermoplastic material through optical and/or mechanical weaknesses [61, 73, 74, 76]. The reasons are mainly based on the insufficient structural orientation of the polymer chains in the weld line region [61, 74, 75, 77, 78]. In the last few years, technologies for injection molding have been developed to change the molecular or fiber orientation in the weld line area and therefore reduce weakness, especially of filled polymer systems. The most effective technologies are push-pull and sequential injection molding [79–81].

Regarding the bonding of PLA to other thermoplastic materials or thermoplastic elastomers in soft-hard combinations, the assembly injection molding (overmolding) has been used in some studies [3]. In this case, the interface occurs by overmolding a hot melt on a cooled surface of a previous injection molded part. The influence of injection molding-induced interfaces on the mechanical behavior

and the specific crystalline structure of PLLA at interfaces were recently investigated at Leibniz-Institut für Polymerforschung Dresden e. V. [59–61, 76]. Depending on the cooling conditions during the process, specific structural gradients are developed at those interfaces, for example, frozen boundary layers.

To gain fundamental information on the bonding behavior of PLA and to compare the different kinds of interfaces, some tensile bars with and without interface were manufactured. In addition to the variation of interface development, the process was performed to induce amorphous or semi-crystalline PLA parts as well as to combine the different structured parts by joining through injection molding (overmolding). For amorphous PLA samples the melt was injected into a cold mold. The semi-crystalline samples were made by molding into a hot mold. The results in Fig. 19 show the comparison of reference samples without interfaces, where the tensile strength is strongly dependent on the crystallinity. Amorphous values are higher than the crystalline ones. In the middle of the diagram (Fig. 19), results for weld line samples are seen with lower values compared to amorphous samples without any interface. Interestingly, the weld line strength is the same for amorphous and semi-crystalline samples, and the average value for crystalline samples with weld lines is slightly higher than in samples without interfaces. It seems that the crystalline structure varies a lot, which is also indicated by a higher standard deviation. Finally, for the overmolding-induced interfaces the tensile strength values drop down to lower values, which is related to the thermal conditions during the bonding development on the cold interface of the overmolded part. Indeed, the crystalline combination has reached a rather high level compared to the drastically reduced strength of amorphous samples with that ‘cold’ interface.

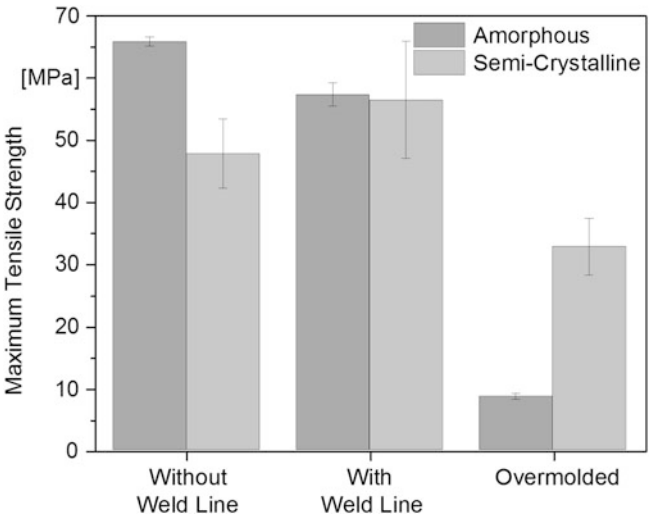

Fig. 19 Maximum tensile strength of injection molded PLA tensile bars without interface, with weld line, and overmolded. (Data source: Leibniz-Institut für Polymerforschung Dresden e. V.)

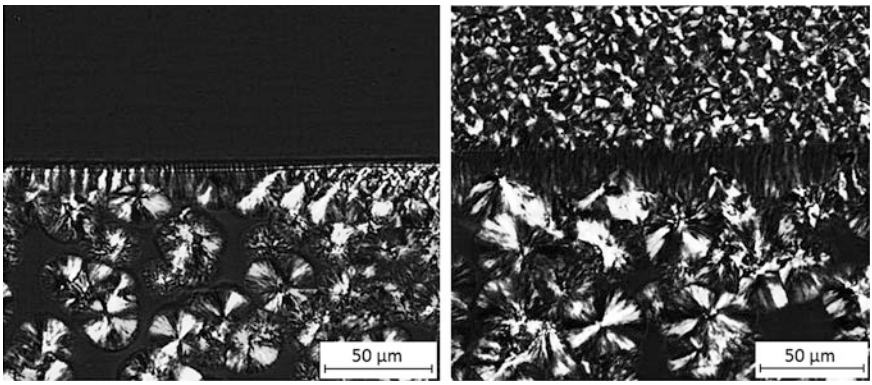

Fig. 20 Polarized light microscopy from overmolded parts: (*left*) overmolded in a cold mold; (*right*) overmolded in a hot mold. (Data source: Leibniz-Institut für Polymerforschung Dresden e. V.)

In Fig. 20 an insight into two different cases of overmolded interfaces with their morphology is given. In the case of the overmolding of amorphous PLA-samples with a hot PLA-melt, the surface is heated and somehow a cold crystallization could take place first. The newly grown crystallites need even more heat to be re-melted. Therefore, the heat flow volume needs to be sufficient for melting and also for initiating bonding mechanisms such as, for example, chain entanglement. In the right micrograph an interface between two crystalline-like PLA moldings was investigated. The second injected part shows a larger spherulite size than the first, which was first injected into a hot mold. Indeed, the second part still remains longer under higher temperature than the first part, which was formed at the mold surface with higher heat conduction coefficient than the PLA and continuously tempered. Figure 21 shows finally a comparison of tensile strength behavior of different semi-crystalline polymers regarding different interfaces through injection molding.

However, the mechanical and thermal properties of injection molded PLA parts are driven by the enormous morphology gradient of the cross section. Common processing conditions (fast cooling, short cycle time) lead to completely amorphous-like molded parts because of the slow crystallization kinetics of PLA. Under processing conditions with high mold temperature, a long residence time in the mold determines the crystallization degree. In turn, this leads to inefficient production. Semi-crystalline parts are only possible to obtain during standard processing cycles if the material contains nucleating agents or blends [1, 2, 14, 55–57].

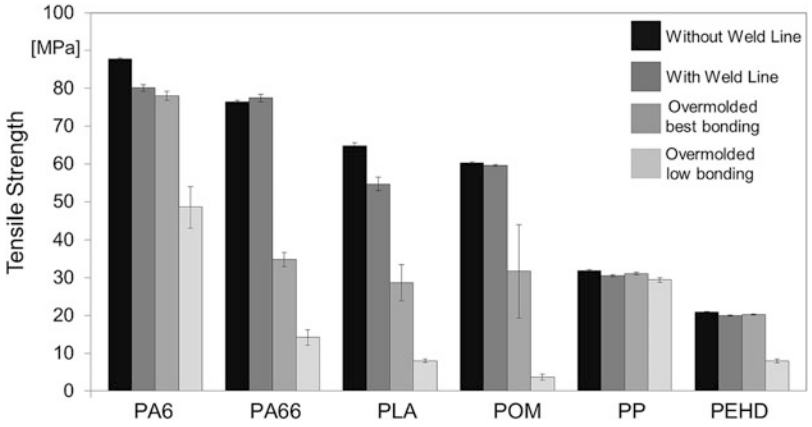

Fig. 21 Tensile strength behavior of semi-crystalline polymers depending on interface formation. (Data source: Leibniz-Institut für Polymerforschung Dresden e. V.)

2.4 Additive Manufacturing

2.4.1 Introduction

In contrast to injection molding or other conventional polymer processing technologies, additive manufacturing (AM) is a relatively new technology and the market for AM is the fastest growing ever seen in the history of industrialization. In 2012 a glorious future for AM was predicted with a value of $4 billion in 2015 and $10.8 billion in 2021 [82]. However, in 2014 the value had already reached $4.1 billion (compound annual growth rate: 35.2%) and is now predicted to reach a value of $21.2 billion by 2020 [83].

AM, formerly known as rapid prototyping and often synonymously described as 3D (three-dimensional) printing, categorizes processes which join materials to make objects from 3D model data, usually layer upon layer [84]. Among all polymer AM processes that utilize thermoplastics, PLA is mostly used in the material extrusion process. The reason is the applicability of the feedstock manufacturing technologies. All powder-based processes, such as binder jetting and powder bed fusion, require completely spherical particles of defined size (<200 µm) and narrow or bi-modal size distribution. So far, no process has been found that generates PLA powder with these characteristics. However, the feedstock for material extrusion technologies is produced by conventional extrusion, where special care needs to be taken to ensure a tight diameter tolerance and circularity of the produced filament with the downstream extrusion equipment. A typically used configuration is an open bath, laser gauge, belt puller, and winder to control these characteristics. However, the use of a vacuum water tank makes the circularity easier to achieve.

2.4.2 Fused Filament Fabrication

In the last few years, material extrusion has become one of the most common AM technologies. It is often referred to as 3D printing, fused deposition modeling (FDM®), fused filament fabrication (FFF), or fused layer manufacturing (FLM). The use of the terminology varies by industry and region. Invented by Stratasys Inc. and commercially available since 1993, FFF is now among the fastest growing AM technologies because of the ease of use, the vast variety of materials, and the range of printers from desktop versions to industrial machines [85]. In most cases the process starts with the creation of a 3D model using computer aided design software. For medical applications and patient-specific models, the 3D data is generated by magnetic resonance imaging or computed tomography scanners where the resulting point cloud is converted to a 3D model. These models are then exported into the STL (STereoLithography) file format, which represents the surface geometry of the part with a mesh of small triangles. This simplified data is then transmitted to the print software and horizontally sliced into different layers depending on the basic print settings. Then the software generates the tool path, which the print head follows. The actual printing process starts by feeding a solid filament through the movement of extrusion gears into a heated nozzle, as shown in Fig. 22. Through heat conduction from the nozzle walls, the material temperature is raised above the melting temperature. The solid filament works as a piston and pushes the molten material out of the tip of the nozzle. These molten beads are then laid down alongside each other, after which they solidify to form a thin horizontal 2D (two-dimensional) layer of polymer. Now either the print head can be raised or the platform can be lowered to print subsequent layers on top of the deposited layer. Hence, complex parts with hollow sections and various surface structures can be easily manufactured. Depending on the part size, the print usually takes several hours.

Two important criteria for FFF printing are the viscosity and heat transfer. The viscosity of the material needs to become low at moderate shear rates to flow out of the

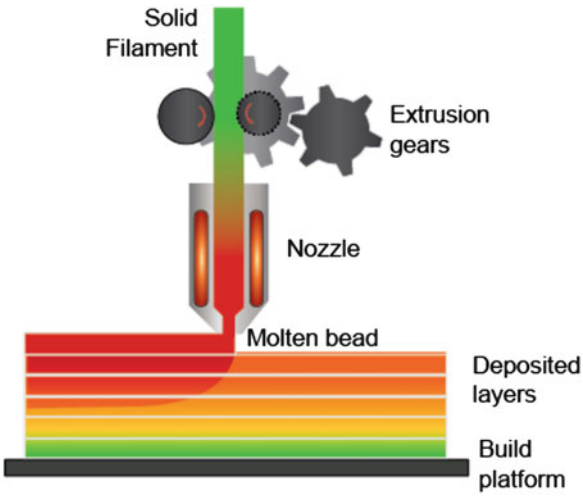

Fig. 22 Schematic of the FFF print process. (Data source: N. Rudolph, Polymer Engineering Center, University of Wisconsin, Madison)

nozzle and rise rapidly upon cooling to avoid sagging of the deposited beads. At the same time, the temperature at the interface still needs to be high enough to allow fusion between beads and layers to occur. Because of the complexity of typical FFF parts, a support structure is needed during printing to prevent overhangs from sagging and to allow for the bridging of long spans. The support structure can either be a break-away support printed with the same material and print head, which is done with most desktop printers, or a water- or detergent-soluble material that is washed out after the print is finished. The latter approach is commonly used for commercial machines with two print heads, and creates smoother surfaces.

PLA is the most commonly used material for desktop or home-user printers. This is because of its low melting temperature in comparison to other filament materials as well as its good adhesion to the build platform and low degree of warpage and delamination. Typical FFF process parameters for PLA are nozzle temperatures of 190–220°C, platform temperatures of RT (room temperature) up to 60°C and print speeds up to 100 mm/s. Another reason for its widespread use in college and community-maker spaces is its low volatile emissions [86].

In commercial printers it is used for applications in the medical and bio-medical industries because of its biocompatibility rather than its mechanical performance. AM in these areas is focused on patient-specific anatomical models and surgery aids, implants containing living cells (bioprinting), scaffolds for tissue engineering, diagnostic platforms, and drug delivery systems [87]. Figure 23 shows a variety of examples.

The requirements range from the macro- to the micro- and nano-levels. For example, the macro-architecture of a scaffold is the overall shape with patient- and organ-specific anatomical features. The microstructure is related to the porosity-like size, shape, and spatial distribution. Finally, the nano-architecture refers to surface modifications that enhance biomolecule adhesion, proliferation, and differentiation. Where the latter is controlled during post-processing, the macro- and micro-

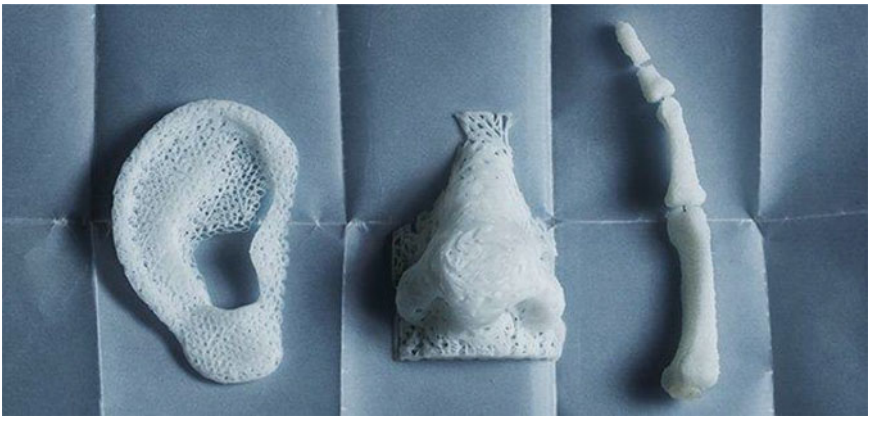

Fig. 23 Ear, nose, and bone scaffolds printed at the Wake Forest Institute for Regenerative Medicine; the PLA scaffolds can be coated with cells to grow body parts [88]. (With permission of Laurie Rubin Photography + Film)

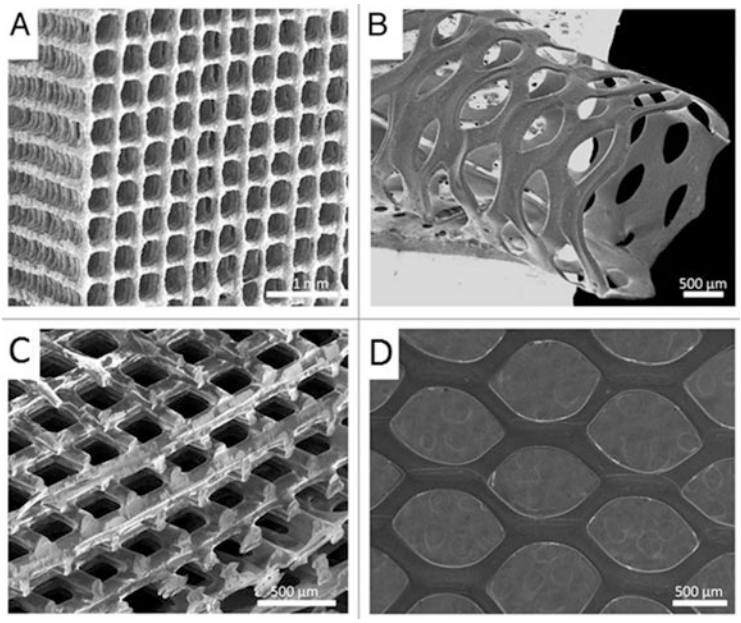

Fig. 24 SEM images of biodegradable 3D structures with PLA and blends: (**a**) PLA/glass composite orthogonal structure; (**b**) PLA tubular hexagonal mesh; (**c**) PLA orthogonal-displaced structure; (**d**) PLA hexagonal mesh [89] (with permission from Taylor and Francis)

architecture is controlled during design and printing. By using fine nozzles of down to 200 µm, the desired microstructure can be obtained. Studies have been carried out using homogeneous PLA polymers [89, 90] as well as blends. In Fig. 24, examples of scaffold microstructures are shown. Blends are used to improve printability and, more importantly, to increase bioactivity. Common blends are PLA/glass composites to improve the mechanical strength and surface roughness. Poly(lactic-*co*-glycolic acid) (PLGA) is used because of its biodegradability and biocompatibility [91]. It is also used as blends: PLGA-TCP [92], PCL-PLGA-TCP [93], and PLGA-PCL [94].

2.4.3 Vat Photopolymerization

Vat photopolymerization (VP), also known as stereolithography, is another AM technology that was only recently used to print with photo-curable poly(D,L-lactide) resin to create scaffold structures [95]. The necessary photo-crosslinking capability is achieved by modification of the end groups to acrylate or methacrylate. The VP process utilizes a vat of liquid photopolymer resin cured by ultraviolet (UV) laser to solidify the pattern layer by layer to create the solid 3D model. The laser beam traces the boundaries and fills in a 2D cross section of the model, solidifying the resin wherever it passes. Each successive layer is applied by submersion of the build platform into the resin. Once the model is complete, the platform rises out of

the vat and the excess resin is drained out of hollow sections. The model is then removed from the platform, excess resin is washed off, and it is then placed in a UV oven for the final curing process. VP parts have excellent surface properties and the highest attainable resolutions. However, the mechanical properties of most parts printed with photo-curable resins degrade over time because of continued exposure to light. However, this potential downfall is not a problem with patient-specific models, which normally have a service life of a couple of hours to a few weeks.

3 Summary

This chapter gives an overview of the processing-related behavior of PLA and the scientific insights of the last few years are reviewed. Common process methods are extrusion, melt spinning, injection molding, and AM. For these methods an overview of the recommended process conditions is given. Because of the similarities in the processing methods of PLA and petroleum-based materials, no extra equipment is necessary to process PLA. PLA is therefore suitable to replace petroleum-based materials. In the last few years, particularly the structural behavior during and after processing of PLA materials has been investigated. The aim is to generate new application fields for PLA materials. Especially in the areas of melt spinning, injection molding, and AM, the advancement in processing technology and the better understanding of the processes themselves have enhanced the application of PLA. For example, the ability to design the surface structure of melt spinning fibers plays an important role in medical applications. Furthermore, the better understanding of the process-structure-properties behavior makes it possible to influence the crystallinity formation, especially at the interface design in injection molded and fused filament fabricated parts. This knowledge makes PLA useful in technical and 3D designed applications.

Acknowledgments The authors thanks the Institute of Textile Machinery and High Performance Material Technology (ITM) and the Technical University in Dresden (TUD) for cooperation and support, especially in the melt spinning process.

References

1. Lim LT, Auras R, Rubino M (2008) Processing technologies for poly(lactic acid). Prog Polym Sci 33(8):820–852
2. Ren J (2010) Processing of PLA in biodegradable poly(lactic acid): synthesis, modification, processing and applications. Springer, Berlin
3. Fachagentur Nachwachsender Rohstoffe (FNR) (2016) Processing of bioplastics – a guideline. Report
4. Jamshidian M, Tehrany EA, Imran M, Jacquot M, Desobry S (2010) Poly-lactic acid: production, applications, nanocomposites, and release studies. Compr Rev Food Sci Food Saf 9 (5):552–571

5. Endres H-J, Siebert-Raths A (2011) Engineering biopolymers :markets, manufacturing, properties and applications. Hanser, Munich
6. Fakirov S (2012) In: Bhattacharyya D, Fakirov S (eds) Synthetic polymer-polymer composites. Hanser, Munich
7. Jiménez A, Peltzer MA, Ruseckaite RA (2015) Poly(lactic acid) science and technology - processing, additives and applications. RSC, Cambridge
8. Garlotta D (2001) A literature review of poly(lactic acid). J Polym Environ 9(2):63–84
9. Saba N, Jawaid M, Al-Othman O (2017) An overview on polylactic acid, its cellulosic composites and applications. Curr Org Synth 14(2):156–170
10. Goebel L, Bonten C (2014) Influence of the phase morphology on the weldability of PLA/PBAT-blends by using butt-welding. In: Alstadt V, Keller JH, Fathi A (eds) Proceedings of PPS-29: The 29th International Conference of the Polymer Processing Society PPS 2014, AIP Conference Proceedings, vol 1593. pp 312–315. https://doi.org/10.1063/1.4873789
11. Gottermann S, Weinmann S, Bonten C, Standau T, Altstadt V (2016) Modified standard polylactic acid (PLA) for extrusion foaming. In: Holzer CH, Payer M (eds) Proceedings of the Regional Conference Graz 2015, Polymer Processing Society PPS, AIP Conference Proceedings, vol 1779. p 060001. https://doi.org/10.1063/1.4965522
12. Yamoum C, Maia J, Magaraphan R (2017) Rheological and thermal behavior of PLA modified by chemical crosslinking in the presence of ethoxylated bisphenol A dimethacrylates. Polym Adv Technol 28(1):102–112
13. Harris AM, Lee EC (2008) Improving mechanical performance of injection molded PLA by controlling crystallinity. J Appl Polym Sci 107(4):2246–2255
14. Srithep Y, Pholharn D, Turng LS, Veang-in O (2015) Injection molding and characterization of polylactide stereocomplex. Polym Degrad Stab 120:290–299
15. Al-Itry R, Lamnawar K, Maazouz A (2012) Improvement of thermal stability, rheological and mechanical properties of PLA, PBAT and their blends by reactive extrusion with functionalized epoxy. Polym Degrad Stab 97(10):1898–1914
16. Kolstad JJ (1996) Crystallization kinetics of poly(L-lactide-co-meso-lactide). J Appl Polym Sci 62(7):1079–1091
17. Iannace S, Nicolais L (1997) Isothermal crystallization and chain mobility of poly(L-lactide). J Appl Polym Sci 64(5):911–919
18. Miyata T, Masuko T (1998) Crystallization behaviour of poly(L-lactide). Polymer 39 (22):5515–5521
19. Di Lorenzo ML (2005) Crystallization behavior of poly(L-lactic acid). Eur Polym J 41(3):569–575
20. Yasuniwa M, Tsubakihara S, Iura K, Ono Y, Dan Y, Takahashi K (2006) Crystallization behavior of poly(L-lactic acid). Polymer 47(21):7554–7563
21. Androsch R, Schick C (2016) Interplay between the relaxation of the glass of random L/D-lactide copolymers and homogeneous crystal nucleation: evidence for segregation of chain defects. J Phys Chem B 120:4522–4528
22. Di Lorenzo ML, Androsch R (2016) Stability and reorganization of alpha-crystals in random L/D-lactide copolymers. Macromol Chem Phys 217(13):1534–1538
23. Sato Y, Inohara K, Takishima S, Masuoka H, Imaizumi M, Yamamoto H, Takasugi M (2000) Pressure-volume-temperature behavior of polylactide, poly(butylene succinate), and poly (butylene succinate-co-adipate). Polym Eng Sci 40(12):2602–2609
24. Pantani R, De Santis F, Sorrentino A, De Maio F, Titomanlio G (2010) Crystallization kinetics of virgin and processed poly(lactic acid). Polym Degrad Stab 95(7):1148–1159
25. Ehrenstein G, Riedel G, Trawiel P (2004) Thermal analysis of plastics - theory and practice. Carl Hanser, Munich
26. Wunderlich B (2005) Thermal analysis of polymeric materials. Springer, Berlin
27. Desantis P, Kovacs AJ (1968) Molecular conformation of poly(S-lactic acid). Biopolymers 6(3):299–306
28. Kalb B, Pennings AJ (1980) General crystallization behavior of poly(L-lactic acid). Polymer 21(6):607–612

29. Ohtani Y, Okumura K, Kawaguchi A (2003) Crystallization behavior of amorphous poly (L-lactide). J Macromol Sci B42(3–4):875–888
30. Di Lorenzo ML, Rubino P, Immirzi B, Luijkx R, Hélou M, Androsch R (2015) Influence of chain structure on crystal polymorphism 5 of poly(lactic acid). Part 2. Effect of molecular mass on the crystal growth rate and semicrystalline morphology. Colloid Polym Sci 293:2459–2467
31. Burnett BB, McDevit WF (1957) Kinetics of spherulite growth in high polymers. J Appl Phys 28(10):1101–1105
32. Androsch R, Iqbal HMN, Schick C (2015) Non-isothermal crystal nucleation of poly (L-lactic acid). Polymer 81:151–158
33. Androsch R, Schick C, Di Lorenzo ML (2017) Kinetics of nucleation and growth of crystals of poly(L-lactic acid). Adv Polym Sci. Springer, Berlin, pp 1–38
34. Kolesov I, Mileva D, Androsch R, Schick C (2011) Structure formation of polyamide 6 from the glassy state by fast scanning chip calorimetry. Polymer 52(22):5156–5165
35. Rhoades AM, Williams JL, Androsch R (2015) Crystallization kinetics of polyamide 66 at processing-relevant cooling conditions and high supercooling. Thermochim Acta 603:103–109
36. Grellmann W, Altstädt V (2007) Polymer testing. Hanser, Munich
37. Osswald TA, Rudolph N (2015) Polymer rheology :fundamentals and applications. Hanser, Munich
38. Auras R, Harte B, Selke S (2004) An overview of polylactides as packaging materials. Macromol Biosci 4(9):835–864
39. Datta R, Henry M (2006) Lactic acid: recent advances in products, processes and technologies - a review. J Chem Technol Biotechnol 81(7):1119–1129
40. Naturworks (2015) Sheet extrusion processing guide. Broshure of Naturworks LLC, Minnetonka
41. Osswald TA, Hernández-Ortiz JP (2006) Polymer processing :modeling and simulation. Hanser Gardner, Munich
42. Corre YM, Duchet J, Reignier J, Maazouz A (2011) Melt strengthening of poly (lactic acid) through reactive extrusion with epoxy-functionalized chains. Rheol Acta 50(7–8):613–629
43. Ljungberg N, Andersson T, Wesslen B (2003) Film extrusion and film weldability of poly(lactic acid) plasticized with triacetine and tributyl citrate. J Appl Polym Sci 88(14):3239–3247
44. Zhou ZF, Huang GQ, Xu WB, Ren FM (2007) Chain extension and branching of poly(L-lactic acid) produced by reaction with a DGEBA-based epoxy resin. Express Polym Lett 1(11):734–739
45. Anderson KS, Hillmyer MA (2004) The influence of block copolymer microstructure on the toughness of compatibilized polylactide/polyethylene blends. Polymer 45(26):8809–8823
46. Ljungberg N, Wesslen B (2002) The effects of plasticizers on the dynamic mechanical and thermal properties of poly(lactic acid). J Appl Polym Sci 86(5):1227–1234
47. Kulinski Z, Piorkowska E (2005) Crystallization, structure and properties of plasticized poly (L-lactide). Polymer 46(23):10290–10300
48. Martin O, Averous L (2001) Poly(lactic acid): plasticization and properties of biodegradable multiphase systems. Polymer 42(14):6209–6219
49. Hagen R (2013) The potential of PLA for the fiber market. Bioplast Mag 8:12ff
50. Schmack G, Tandler B, Optiz G, Vogel R, Kornber H, Haussler L, Voigt D, Weinmann S, Heinernann M, Fritz HG (2004) High-speed melt spinning of various grades of polylactides. J Appl Polym Sci 91(2):800–806
51. Perepelkin K (2002) Chemistry and technology of chemical fibres – polylactid fibers: fabrication, properties, use, prospects. Fiber Chem 34(2):85–100
52. Beyreuther R, Brünig H (2007) Dynamics of fibre formation and processing :modelling and application in fibre and textile industry. Springer, Berlin
53. Hahn J, Breier A, Brünig H, Heinrich G (2016) Mechanical adapted embroidered scaffolds based on polylactic acid melt spun multifilaments for ligament tissue engineering. Annual report of Leibniz-Institut für Polymerforschung Dresden e. V., Dresden. chapter: Biology-inspired interface and material design. pp. 42–44. http://www.ipfdd.de/en/publications/annual-reports/. Comment: The source is from the Leibniz-Institut für Polymerforschung Dresden e.V.

54. Tran NHA, Brünig H, Hinüber C, Heinrich G (2014) Melt spinning of biodegradable nanofibrillary structures from poly(lactic acid) and poly (vinyl alcohol) blends. Macromol Mater Eng 299(2):219–227
55. Ghosh S, Viana JC, Reis RL, Mano JF (2007) Effect of processing conditions on morphology and mechanical properties of injection-molded poly(L-lactic acid). Polym Eng Sci 47(7):1141–1147
56. Ghosh S, Viana JC, Reis RL, Mano JF (2008) Oriented morphology and enhanced mechanical properties of poly(L-lactic acid) from shear controlled orientation in injection molding. Mater Sci Eng A 490(1–2):81–89
57. Siebert-Raths A (2012) Modifizierung von polylactid (PLA) für technische Anwendungen, Verfahrenstechnische Optimierung der Verarbeitungs- und Gebrauchseigenschaften. Dissertation, Hannover
58. Kuehnert I (2009) Cold and hot interfaces during injection molding. In: PPS-25 Polymer Processing Society. Goa, Indien
59. Kuehnert I, Pompsch I (2011) Morphology and strength of injection molded parts with interfaces. In: Proceedings of SPE Antec 2011, Society of Plastics Engineers, Bosten
60. Kuehnert I, Schoenfeldt A, Auf der Landwehr M (2013) New insights into interfaces in injection molded parts. In: Proceedings of SPE Antec 2013, Society of Plastics Engineers, Cincinnati
61. Kuehnert I, Spoerer Y, Zimmermann M (2016) Weld lines in injection molded parts: strength, morphology and improvement. In: Proceedings of SPE Antec 2016, Society of Plastics Engineers, Indianapolis
62. Market study and Database on Bio-based Polymers in the World – Capacity, Production and Applications: Status Quo and Trends towards 2020. 2013–7; Nova-Institut GmbH, Chemiepark Knapsack, Industriestraße 300, 50354 Huerth Germany
63. Sundar V (2012) Manufacture and characterization of filament yarns with structured and collagen-coated surfaces for medical purposes. TU-Dresden and Leibniz-Institut für Polymerforschung Dresden e.V
64. Akram W (2015) Manufacturing and characterization of high-oriented, low-shrinkage and biodegradable filament yarns for medical applications. TU-Dresden and Leibniz-Institut für Polymerforschung Dresden e.V
65. Hahner J, Hinuber C, Breier A, Siebert T, Brunig H, Heinrich G (2015) Adjusting the mechanical behavior of embroidered scaffolds to lapin anterior cruciate ligaments by varying the thread materials. Text Res J 85(14):1431–1444
66. Hahn J, Breier A, Brünig H, Heinrich G (2017) Long-term hydrolytic degradation study on polymer-based embroidered scaffolds for ligament tissue engineering. J Ind Text 804:1–16
67. Tran NHA, Brunig H, Auf der Landwehr M, Heinrich G (2016) Controlling micro- and nanofibrillar morphology of polymer blends in low-speed melt spinning process. Part III: Fibrillation mechanism of PLA/PVA blends along the spinline. J Appl Polym Sci 133(48):16
68. Tran N (2016) Melt spinning and characterization of biodegradable micro- and nanofibrillar structures from poly(lactic acid) and poly(vinyl alcohol) blends. PhD-Thesis. TU-Dresden and Leibniz-Institut für Polymerforschung Dresden e.V. TUD Press. ISBN: 978-3-95908-051-4
69. Kamal M, Isayev I, Liu SJ (2009) Injection molding-technology and fundamentals. Hanser, Munich
70. Battegazzore D, Bocchini S, Frache A (2011) Crystallization kinetics of poly(lactic acid)-talc composites. Express Polym Lett 5(10):849–858
71. Yin YG, Zhang XQ, Song Y, de Vos S, Wang RY, Joziasse CAP, Liu GM, Wang DJ (2015) Effect of nucleating agents on the strain-induced crystallization of poly(L-lactide). Polymer 65:223–232
72. Jing ZX, Shi XT, Zhang GC (2016) Rheology and crystallization behavior of asymmetric PLLA/PDLA blends based on linear PLLA and PDLA with different structures. Polym Adv Technol 27(8):1108–1120
73. Malguarnera SC (1982) Weld lines in polymer processing. Polym-Plast Technol Eng 18(1):1–45

74. Mennig G (1995) Knit-line behaviour of polypropylene and polypropylene-blends. Polypropylene: structure, blends and composites, vol 1. Chapman & Hall, London, pp 205–226
75. Nguyen-Chung T, Plichta C, Mennig G (1998) Flow disturbance in polymer melt behind an obstacle. Rheol Acta 37(3):299–305
76. Fischer M, Ausias G, Kuehnert I (2016) Investigation of interfacial fracture behavior on injection molded parts. In: Rhee B (ed) Proceedings of PPS-31: The 31st International Conference of the Polymer Processing Society PPS 2015, AIP Conference Proceedings. vol 1713. pp 040011. https://doi.org/10.1063/1.4942276
77. Haufe A, Kuehnert I, Mennig G (1999) Zum Einfluss strömungsinduzierter Fehlerstellen auf das Versagensverhalten in spritzgegossenen Kunststoffbauteilen. GAK 4:354–358
78. Kuehnert I (2005) Grenzflächen beim Mehrkunststoff-Spritzgießen. Dissertation, Fakultät Maschinenbau. TU-Chemnitz, Hanser:Munich. http://archiv.tu-chemnitz.de/pub/2005/0166/data/Diss_Kuehnert.pdf or https://kunststoffe.de/fachinformationen/dissertationen/artikel/grenzflächen-beim-mehrkunststoffspritzgiessen-640067.html
79. Gutjahr L, Becker H (1989) Herstellen technischer Formteile mit dem Gegentaktspritzgießverfahren. Kunststoffe 79(11):1108–1112
80. Malloy RA (2011) Plastic part design for injection molding: an introduction, 2 edn. Hanser, Munich
81. Kuehnert I, Vetter K (2008) Sequential injection moulding as a method for eliminating weld lines - praxis and simulation. RFP 3(5):256–261
82. Wohlers T (2013) Wohlers report 2013: additive manufacturing and 3D printing: state of the industry: annual worldwide progress report
83. Wohlers T (2015) Wohlers report 2015: additive manufacturing and 3D printing: state of the industry: annual worldwide progress report
84. ASTM F2792-12a Standard Terminology for Additive Manufacturing Technologies (Withdrawn 2015) (2012) ASTM International West Conshohocken PA
85. Gebhardt A (2011) Understanding additive manufacturing :rapid prototyping, rapid tooling, rapid manufacturing. Hanser, Munich
86. McDonnell B, Guzman X, Doblack M, Simpson T, and Cimbala J Cimbala JM (2016) 3D printing in the wild, a preliminary, investigation of air quality in college maker spaces. In: 27th Annual International Solid Freeform Fabrication Symposium. Austin, TX, USA
87. Chia HN, Wu BM (2015) Recent advances in 3D printing of biomaterials. J Biol Eng 9:14
88. Royte E (2013) What lies ahead for 3-D printing? The new technology promises a factory in every home – and a whole lot more. Smithonian Magazine. http://www.smithsonianmag.com/science-nature/what-lies-ahead-for-3-d-printing-37498558/?all
89. Serra T, Mateos-Timoneda MA, Planell JA, Navarro M (2013) 3D printed PLA-based scaffolds A versatile tool in regenerative medicine. Organogenesis 9(4):239–244
90. Korpela J, Kokkari A, Korhonen H, Malin M, Narhi T, Seppala J (2013) Biodegradable and bioactive porous scaffold structures prepared using fused deposition modeling. J Biomed Mater Res B Appl Biomater 101B(4):610–619
91. Yen HJ, Tseng CS, Hsu SH, Tsai CL (2009) Evaluation of chondrocyte growth in the highly porous scaffolds made by fused deposition manufacturing (FDM) filled with type II collagen. Biomed Microdevices 11(3):615–624
92. Kim J, McBride S, Tellis B, Alvarez-Urena P, Song YH, Dean D (2012) Rapid-prototyped PLGA/β-TCP/hydroxyapatite nanocomposite scaffolds in a rabbit femoral defect model. Biofabrication 4:025003
93. Shim JH, Moon TS, Yun MJ, Jeon YC, Jeong CM, Cho DW, Huh JB (2012) Stimulation of healing within a rabbit calvarial defect by a PCL/PLGA scaffold blended with TCP using solid freeform fabrication technology. J Mater Sci Mater Med 23(12):2993–3002
94. Kim JY, Cho DW (2009) Blended PCL/PLGA scaffold fabrication using multi-head deposition system. Microelectron Eng 86(4-6):1447–1450
95. Melchels FPW, Feijen J, Grijpma DW (2009) A poly(D,L-lactide) resin for the preparation of tissue engineering scaffolds by stereolithography. Biomaterials 30(23–24):3801–3809